

# DS-7300a, a DNA Topoisomerase I Inhibitor, DXd-Based Antibody–Drug Conjugate Targeting B7-H3, Exerts Potent Antitumor Activities in Preclinical Models



Michiko Yamato<sup>1</sup>, Jun Hasegawa<sup>1</sup>, Takanori Maejima<sup>1</sup>, Chiharu Hattori<sup>1</sup>, Kazuyoshi Kumagai<sup>1</sup>, Akiko Watanabe<sup>1</sup>, Yumi Nishiya<sup>1</sup>, Tomoko Shibutani<sup>2</sup>, Tetsuo Aida<sup>1</sup>, Ichiro Hayakawa<sup>1</sup>, Takashi Nakada<sup>1</sup>, Yuki Abe<sup>1</sup>, and Toshinori Agatsuma<sup>1</sup>

## ABSTRACT

B7-H3 is overexpressed in various solid tumors and has been considered as an attractive target for cancer therapy. Here, we report the development of DS-7300a, a novel B7-H3–targeting antibody–drug conjugate with a potent DNA topoisomerase I inhibitor, and its *in vitro* profile, pharmacokinetic profiles, safety profiles, and *in vivo* antitumor activities in nonclinical species.

The target specificity and species cross-reactivity of DS-7300a were assessed. Its pharmacologic activities were evaluated in several human cancer cell lines *in vitro* and xenograft mouse models, including patient-derived xenograft (PDX) mouse models *in vivo*. Pharmacokinetics was investigated in cynomolgus monkeys. Safety profiles in rats and cynomolgus monkeys were also assessed.

DS-7300a specifically bound to B7-H3 and inhibited the growth of B7-H3–expressing cancer cells, but not that of B7-H3–negative

cancer cells, *in vitro*. Additionally, treatment with DS-7300a and DXd induced phosphorylated checkpoint kinase 1, a DNA damage marker, and cleaved PARP, an apoptosis marker, in cancer cells. Moreover, DS-7300a demonstrated potent *in vivo* antitumor activities in high–B7-H3 tumor xenograft models, including various tumor types of high–B7-H3 PDX models. Furthermore, DS-7300a was stable in circulation with acceptable pharmacokinetic profiles in monkeys, and well tolerated in rats and monkeys.

DS-7300a exerted potent antitumor activities against B7-H3–expressing tumors in *in vitro* and *in vivo* models, including PDX mouse models, and showed acceptable pharmacokinetic and safety profiles in nonclinical species. Therefore, DS-7300a may be effective in treating patients with B7-H3–expressing solid tumors in a clinical setting.

## Introduction

B7-H3, also known as CD276, is a type I transmembrane protein belonging to the B7 family that includes immune checkpoint molecules such as PD-L1, B7-1, and B7-2 (1, 2). Human B7-H3 has two isoforms: one has a single pair of immunoglobulin (Ig) variable (V)-like and Ig constant (IgC)-like domains in the extracellular region (2Ig B7-H3) and the other has two pairs of IgV-IgC domains (4Ig B7-H3), whereas mouse B7-H3 has only one isoform (2Ig B7-H3). It has been reported that 4Ig B7-H3 is the dominant isoform in human tissues (3–6). B7-H3 is highly expressed on various types of human solid cancers including lung, esophageal, endometrial, prostate, and breast cancers. Several studies have also reported that B7-H3 overexpression was correlated with poor prognosis in various types of cancers (7–13). In tumor tissues, B7-H3 is expressed in tumor cells and tumor stromal cells such as tumor vascular endothelial cells, pericytes, and fibroblasts (14, 15).

In normal human tissues, B7-H3 expression is broadly observed at the mRNA level, but protein expression is limited and remains at relatively low levels in the organs such as liver, colon, ovary, and prostate (1, 14, 16, 17). Some physiologic functions of B7-H3 have been reported. It was identified as a costimulatory molecule of T-cell function (1). On the other hand, recent evidence suggests that B7-H3 is a coinhibitory molecule and promote tumorigenesis by regulating tumor-infiltrating immune cells (6). In addition, B7-H3 plays a role in cancer progression, migration, invasion, antiapoptosis, metabolic reprogramming, and angiogenesis (6, 18). However, no counter-receptors of B7-H3 have been identified. Recently, the IL20 receptor subunit  $\alpha$  (IL20RA) has been reported as a putative binding partner for B7-H3 (19), but the role of B7-H3 in IL20RA-expressing cells is still unknown. Although the physiologic functions of B7-H3 remain to be fully elucidated, it is expected to be an attractive target for anticancer therapies due to its expression profiles and epidemiologic data. Several treatment modalities targeting B7-H3, such as enhanced antibody-dependent cellular cytotoxicity (ADCC) antibodies, CD3-bispecific antibodies, chimeric antigen receptor (CAR)-T cells, and antibody–drug conjugates (ADC), have been under development (6, 17, 20–23); however, no B7-H3–targeting therapeutic agents have been approved to date.

ADCs, composed of an mAb, linker, and biologically active payload such as cytotoxic drugs, are designed to exert potent antitumor activity against the target-expressing cancer cells by delivering the payload into the cells in a target-dependent manner (24). Therefore, they have the potential for a wide therapeutic window with reduced off-target systemic toxicity. Several ADCs have been approved and a large number of clinical studies for new ADCs are currently ongoing (24). Recently, a unique linker-payload technology platform, DXd-ADC technology, has been developed which consists of an enzymatically

<sup>1</sup>Daiichi Sankyo Co., Ltd., Tokyo, Japan. <sup>2</sup>Daiichi Sankyo RD Novare Co., Ltd., Tokyo, Japan.

**Note:** Supplementary data for this article are available at Molecular Cancer Therapeutics Online (<http://mct.aacrjournals.org/>).

**Corresponding Author:** Michiko Yamato, Daiichi Sankyo Co., Ltd., 1-2-58, Hiromachi, Shinagawa-ku, Tokyo 140-8710, Japan. Phone: 81-3-3492-3131; E-mail: [yamato.michiko.kg@daiichisankyo.co.jp](mailto:yamato.michiko.kg@daiichisankyo.co.jp)

Mol Cancer Ther 2022;21:635–46

doi: 10.1158/1535-7163.MCT-21-0554

This open access article is distributed under Creative Commons Attribution-NonCommercial-NoDerivatives License 4.0 International (CC BY-NC-ND).

©2022 The Authors; Published by the American Association for Cancer Research

cleavable tetra-peptide-based linker and a novel exatecan derivative (DXd) payload (25–27). DXd is a more potent DNA topoisomerase I (TOP1) inhibitor than SN-38, an active metabolite of irinotecan (26). The DXd-ADC technology has a linker stable in plasma, a payload with a short systemic half-life, and an ADC in which the average drug-to-antibody ratio (DAR) can be optimized to up to 8 for each target (25–30). A novel HER2-targeting ADC, trastuzumab deruxtecan, to which the DXd-ADC technology was applied, has been reported to exhibit potent antitumor activities in preclinical models (26, 31). T-DXd also showed robust efficacy in clinical trials (32–38) and has recently been approved in the United States, Japan, the EU, and the UK for the treatment of adult patients with unresectable or metastatic HER2-positive breast cancer who have received two or more prior anti-HER2-based regimens in the metastatic setting, and in Japan and the United States for the treatment of adult patients with HER2-positive unresectable advanced or recurrent gastric cancer that has progressed after a trastuzumab-containing regimen. Further, the DXd-ADC technology has been applied to other targets for cancer therapy and several DXd-ADC programs are under clinical development (28–30).

We generated DS-7300a, a novel B7-H3-targeting ADC, using DXd-ADC technology, which is composed of a humanized anti-B7-H3 mAb, an enzymatically cleavable tetra-peptide-based linker, and a potent TOP1 inhibitor, DXd. DS-7300a is designed to bind to B7-H3 on the cell surface; upon binding, it is internalized into cancer cells and releases its DXd in cytoplasm after its linker is being cleaved with enzymatic processing. The released DXd inhibits TOP1 activity and leads to the apoptosis of target cancer cells. In this article, we describe the nonclinical profiles of DS-7300a, including pharmacologic activities, pharmacokinetics, and safety profiles in nonclinical species.

## Materials and Methods

### Antibodies and ADCs

The parental anti-B7-H3 antibody (Ab), a humanized IgG1 mAb, was generated by humanization of the mouse anti-human B7-H3 mAb, which was obtained by the immunization of mice with human breast adenocarcinoma MCF-7 cells (20). DS-7300a was produced in accordance with the procedure published previously (25, 26), conjugating exatecan derivative-based cytotoxic payload DXd to the parental anti-B7-H3 Ab. The drug distribution was analyzed by hydrophobic interaction chromatography. The isotype control ADC was produced in the same manner as DS-7300a with a comparable DAR.

### IHC analysis of B7-H3 expression

Human tumor tissue microarrays (TMA) were provided from University Hospital Basel, Switzerland. *In vivo* xenograft tumor samples were collected from untreated xenograft model mice. The tumor samples were fixed in 10% neutral buffered formalin and embedded in paraffin, and 4- $\mu$ m-thick tissue sections were used for IHC using BenchMark ULTRA (Ventana Medical Systems, Inc.). The slides were deparaffinized and incubated in Tris-based antigen retrieval solution (CC1) for 32 minutes at 100°C. Then, the slides were sequentially incubated with anti-human B7-H3 mAb (Daiichi Sankyo, final concentration of 5  $\mu$ g/mL) as a primary antibody for 24 minutes at 36°C, and OptiView Universal DAB Kit with anti-Rb HQ (RRID: AB\_2833075) was used according to the manufacturer's instructions. The slides were finally counterstained with hematoxylin and mounted. Whole slide images were captured by NanoZoomer-XR (Hamamatsu Photonics) and H-score was calculated using the HALO image analysis

software (Indica Labs):  $H\text{-score} = (3 \times \% \text{ tumor cells with strong membrane staining}) + (2 \times \% \text{ tumor cells with moderate membrane staining}) + (1 \times \% \text{ tumor cells with weak membrane staining})$ . The *H*-score could range from 0 to 300.

### Cell lines

The human acute lymphocytic leukemia cell line CCRF-CEM (RRID:CVCL\_0207), the human lung adenocarcinoma cell line Calu-6 (RRID:CVCL\_0236), and the Chinese hamster ovary cell line CHO-K1 (RRID:CVCL\_0214) were purchased from ATCC. The human rhabdomyosarcoma cell line RH-41 (RRID:CVCL\_2176) and human endometrial adenocarcinoma cell line MFE-280 (RRID: CVCL\_1405) were purchased from the Leibniz Institute DSMZ (Braunschweig, Germany). All of the cells were cultured with appropriate media supplemented with 10% heat-inactivated FBS [minimum essential medium (MEM) for Calu-6, RPMI1640 Medium for RH-41 and CCRF-CEM, Ham F-12K (Kaighn) Medium for CHO-K1], or 20% heat-inactivated FBS [RPMI 1640 Medium/MEM for MFE-280 supplemented with 1  $\times$  insulin, transferrin, and selenium (ITS)] at 37°C in a humidified atmosphere containing 5% CO<sub>2</sub>. All cell lines were authenticated by short tandem repeat profiling and were routinely tested for *Mycoplasma* by PCR. Cells were used within 10 passages after thawing.

### ELISA

Immunoplates were coated with recombinant C-terminal His-tagged human B7 family proteins, 0.05  $\mu$ g/mL hB7-H1 (PD-L1), hB7-H2, hB7-H3 (4Ig), hB7-H5, hB7-H6, hB7-1, hB7-2, and hPD-L2 or 0.2  $\mu$ g/mL hB7-H4 overnight at 4°C, washed, blocked with 1% BSA, and then incubated with 40  $\mu$ g/mL DS-7300a or isotype control ADC for 1 hour at 22°C. All of the human B7 family proteins were purchased from R&D Systems. Anti-His (RRID:AB\_11204427) and isotype control (RRID:AB\_2891079) antibodies (BioLegend, Inc.) were also used as positive and negative controls, respectively. After washing, horseradish peroxidase (HRP)-conjugated anti-human IgG antibody (RRID:AB\_2337596, Jackson ImmunoResearch Laboratories, Inc.) for the detection of DS-7300a and isotype control ADC, or HRP-conjugated anti-mouse IgG antibody (RRID:AB\_92581, Merck KGaA) for the detection of anti-His and isotype control antibodies were added and incubated for another hour. After washing, 3,3',5,5'-tetramethylbenzidine (TMB) soluble reagent (ScyTek Laboratories, Inc.) was added and then the reaction was stopped by addition of TMB stop buffer (ScyTek Laboratories, Inc.). The absorbance at 450 nm was measured using a microplate reader, Infinite M200 PRO (TECAN Austria GmbH).

### Cell-based ELISA

The cross-reactivity of DS-7300a with the other human B7 family proteins, hHHLA2 and hBTNL2, was evaluated by cell-based ELISA. CHO-K1 cells were transiently transfected with expression plasmid vectors encoding N-terminal FLAG-tagged human B7 family proteins, hB7-H3 (4Ig), hHHLA2, and hBTNL2, and a mock plasmid vector as a negative control in a collagen-coated plate and incubated overnight at 37°C in a humidified atmosphere containing 5% CO<sub>2</sub>. The transfected cells were incubated with PBS containing 50% FBS for 45 minutes at 37°C in a humidified atmosphere containing 5% CO<sub>2</sub> and then incubated with 40  $\mu$ g/mL DS-7300a for 1 hour at 4°C. Anti-FLAG antibody (RRID:AB\_1134266, BioLegend, Inc., 4  $\mu$ g/mL) was also used to confirm the protein expression. After washing, HRP-conjugated anti-human IgG antibody for DS-7300a or HRP-conjugated anti-rat IgG antibody (RRID:AB\_2338144, Jackson ImmunoResearch

Laboratories, Inc.) for anti-FLAG antibody was added and incubated for another hour at 4°C. After washing, TMB soluble reagent was added and then the reaction was stopped by addition of TMB stop buffer. The absorbance at 450 nm was measured using Infinite M200 PRO. The species cross-reactivity and the binding affinity of DS-7300a to cynomolgus monkey, rat, and mouse B7-H3 proteins were also evaluated by cell-based ELISA. CHO-K1 cells were transiently transfected with expression plasmid vectors encoding *N*-terminal FLAG-tagged B7-H3 orthologs, human B7-H3 (4Ig and 2Ig), cynomolgus monkey B7-H3 (4Ig and 2Ig), rat B7-H3, and mouse B7-H3 in a collagen-coated plate and incubated overnight at 37°C in a humidified atmosphere containing 5% CO<sub>2</sub>. The transfected cells were incubated with serially diluted DS-7300a for 1 hour at 4°C. Anti-FLAG antibody (4 µg/mL) was also used to confirm the protein expression. After washing, HRP-conjugated anti-human IgG antibody for DS-7300a or HRP-conjugated anti-rat IgG antibody for anti-FLAG antibody was added and incubated for another hour at 4°C. After washing, TMB soluble reagent was added and then the reaction was stopped by addition of TMB stop buffer. The absorbance at 450 nm was measured using Infinite M200 PRO. The EC<sub>50</sub> value calculated by a sigmoid E<sub>max</sub> model was defined as the dissociation constant (K<sub>d</sub>) value that indicates the binding affinity of DS-7300a.

#### **In vitro stability in plasma**

The release rate of DXd from 100 µg/mL DS-7300a in mouse, rat, monkey, and human plasma and buffer containing 1% BSA was evaluated at 37°C for up to 21 days. Plasma and buffer samples were deproteinized with ethanol and then analyzed by LC-MS/MS (LC, Shimadzu; MS, AB SCIEX). The release rate of DXd was calculated using the mean concentration of DXd (*N* = 3).

#### **Flow cytometry**

For the B7-H3 expression analysis in each cell line, cells were stained with PE-conjugated anti-human B7-H3 antibody (anti-B7-H3-PE, RRID:AB\_10831020, Miltenyi Biotec Inc.) or PE-conjugated isotype control antibody (mIgG2b-PE, RRID:AB\_2661750, Miltenyi Biotec Inc.) on ice for 30 minutes in the dark. The cells were washed, and the fluorescence intensity of each stained cell was measured by a flow cytometer (Becton, Dickinson, and Company, FACSCanto II).

#### **Cytotoxicity assay**

Cells were seeded into 96-well low-cell-adhesion cell culture plates at 2,000 cells per well. After overnight incubation, each serially diluted test substance (DS-7300a, parental anti-B7-H3 Ab, isotype control ADC, and DXd) was added then all of the plates were incubated for 6 days. After the incubation, cell viability was evaluated using 3D Cell Viability Assay (Promega Corp.) in accordance with the manufacturer's instructions. The luminescence was measured by a microplate reader, ARVO X3 (PerkinElmer Japan Co., Ltd.). The concentration of each substance inducing 50% inhibition (IC<sub>50</sub>) in each cell line was estimated in accordance with the sigmoid E<sub>max</sub> model.

#### **Western blotting**

RH-41 cells were treated with 10 µg/mL DS-7300a, parental anti-B7-H3 Ab, isotype control ADC, or 10 nmol/L DXd for 72 hours. The cells were washed, collected, and then lysed in RIPA buffer supplemented with Halt protease and phosphatase inhibitor cocktail (Thermo Fisher Scientific Inc.). The lysates were collected after centrifugation at 21,500 × *g* for 10 minutes at 4°C, and their protein concentration was quantified using Pierce BCA Protein Assay

(Thermo Fisher Scientific Inc.). Equal amounts of proteins were subjected to Simple Western analysis using the Wes System (ProteinSimple Japan K.K.), in accordance with the manufacturer's instructions. In brief, cell lysates were mixed with master mix and heated at 95°C for 5 minutes. The samples, biotinylated ladder, anti-checkpoint kinase 1 (Chk1) antibody (RRID:AB\_627257, Santa Cruz Biotechnology, Inc.), anti-phosphorylated Chk1 (Ser317) antibody (RRID:AB\_2783865), anti-cleaved PARP (Asp214) antibody (RRID:AB\_331426), and anti-β-actin antibody (RRID:AB\_2242334) (Cell Signaling Technology, Inc.), HRP-conjugated secondary antibodies (RRID:AB\_2860576 and RRID:AB\_2860577), streptavidin-HRP, chemiluminescent substrate (ProteinSimple Japan K.K.), and wash buffer were loaded into the microplates containing separation and stacking matrices. After microplate loading, the separation electrophoresis and immunodetection steps were conducted in the capillary system of the Wes System. The measurement was performed using Wes System software, Compass for SW (ProteinSimple Japan K.K.).

#### **Animal studies**

All animal experiments performed in this study were approved by the Institutional Animal Care and Use Committee at Daiichi Sankyo Co., Ltd.

#### **Xenograft studies**

##### **Cancer cell-line-derived xenograft studies**

RH-41 and MFE-280 models were established by injecting 5 × 10<sup>6</sup> cells suspended in Matrigel/DPBS (1:1), while a Calu-6 model was established by injecting 3 × 10<sup>6</sup> cells suspended in saline, subcutaneously into female CAnN.Cg-Foxn1<sup>tm1.1</sup>/CrJ mice (Charles River Laboratories Japan, Inc.), respectively.

#### **PDX studies**

CTG-2093, CTG-0166, CTG-0820, and CTG-1061 studies were performed by Champions Oncology, Inc. Models were established by inoculating tumor fragments derived from patients with small cell lung cancer (SCLC), non-small cell lung cancer (NSCLC), head and neck cancer, and bladder cancer, respectively, which were maintained in host mice, subcutaneously into female Hsd: Athymic Nude-Foxn1<sup>tm1.1</sup> mice (Envigo).

Group assignment was carried out when the tumor volume reached approximately 100 to 300 mm<sup>3</sup>. The tumor-bearing mice were treated with DS-7300a or relevant controls intravenously on days 0 and 14. The tumor volume defined as 0.5 × length × width<sup>2</sup> (cell-line-derived xenograft models) or 0.52 × length × width<sup>2</sup> (PDX models) and the body weight were measured twice a week. The antitumor activity was evaluated on day 28 (in the case of the CTG-1061 model, on day 22), where tumor growth inhibition (TGI, %) was calculated according to the following equation: 100 × [1 - (average tumor volume of the treatment group)/(average tumor volume of the vehicle control group)]. Tumor volumes were compared between the vehicle control group and the treatment groups. The vehicle control group was administered 10 mmol/L acetate buffer (pH5.5) containing 5% sorbitol or 10 mmol/L histidine buffer (pH5.9) containing 9% sucrose and 0.02% polysorbate 20.

#### **Pharmacokinetic study in monkeys**

DS-7300a was administered once intravenously at 0.3, 1, 3, and 10 mg/kg to male cynomolgus monkeys. Plasma concentration of DS-7300a, total antibody (drug conjugated and unconjugated antibody), and DXd were measured up to 28 days post dose, and determined by a ligand binding assay using Gyrolab xP workstation

(Gyros Protein Technologies AB) for DS-7300a and total antibody, and LC-MS/MS for DXd, respectively. Below lower limit of quantification (BLQ) for DS-7300a and total antibody: < 0.100 µg/mL, BLQ for DXd: < 0.100 ng/mL. The pharmacokinetic parameters were calculated by noncompartmental analysis with Phoenix Win-Nonlin (Ver. 6.4, Certara).

### Toxicity studies in rats and monkeys

DS-7300a was intravenously administered once every 2 weeks (three times in total) to Crl:CD(SD) rats, the non-cross-reactive species to DS-7300a, or cynomolgus monkeys, the cross-reactive species. Clinical signs, body weight, food consumption, clinical pathology, and peripheral blood lymphocyte subsets were monitored throughout the study. Necropsy was performed on the day after the last administration, along with histopathologic analysis. The reversibility of the toxic changes was assessed in a subsequent 2-month recovery period in both rats and monkeys.

### Statistical analysis

All statistical analyses except for in the toxicity studies were performed using SAS System Release 9.2 (SAS Institute Inc.). Statistical analysis in the toxicity studies was performed using MiTOX System (Mitsui Zosen Systems Research Inc.). All EC<sub>50</sub> and IC<sub>50</sub> values with 95% confidence interval (CI) were determined by a sigmoid E<sub>max</sub> model. Dunnett multiple comparison tests were used to compare the vehicle control group and the treatment groups in cell-line-derived xenograft model studies, and unpaired *t* test was used to compare the vehicle group and the treatment group in PDX model studies.

### Data availability statement

The data generated in this study are available within the article and its supplementary data files.

## Results

### Expression profile of B7-H3 in solid tumors

To investigate the expression profile of B7-H3 in solid tumors, we performed IHC analysis of B7-H3 expression on human solid tumor TMAs (Fig. 1; Supplementary Fig. S1). In tumor tissues, positive staining of B7-H3 was observed in the tumor cells as well as in the vasculature/endothelium and fibrous stromal cells (Fig. 1A), and B7-H3 was expressed on various types of solid tumors (Fig. 1B). Furthermore, we analyzed the B7-H3 expression levels of *H*-score of the tumor cells across various tumor types in the TMAs. A high frequency of high *H*-scores of B7-H3 expression was observed in various types of solid tumors, including melanoma, endometrial cancer, squamous NSCLC, and bladder cancer (Fig. 1C).

### Characterization of DS-7300a

A schematic structure of DS-7300a is shown in Fig. 2A. DXd was conjugated with anti-B7-H3 mAb via a tetra-peptide-based linker to reduced cysteine residues of the mAb. DS-7300a is designed to release the DXd payload after proteolytic cleavage of the linker by lysosomal enzymes such as cathepsins (26). The DAR of DS-7300a is 4 on average.

To confirm the target specificity of DS-7300a, we assessed its binding activity to human B7 family proteins by ELISA and cell-based ELISA. DS-7300a bound to human B7-H3, but no binding was detected to other human B7 family proteins B7-H1, B7-H2, B7-H4, B7-H5, B7-H6, B7-1, B7-2, and PD-L2 in ELISA (Fig. 2B; Supplementary Fig. S2A). DS-7300a also bound to human B7-H3-transfected

CHO-K1 cells, but not to other human B7 family proteins HHLA2- and BTNL2-transfected CHO-K1 cells in cell-based ELISA (Fig. 2C; Supplementary Fig. S2B). These results indicate that DS-7300a specifically binds to human B7-H3 but does not cross-react with the other human B7 family proteins. Furthermore, we assessed the species cross-reactivity of DS-7300a by cell-based ELISA using human, cynomolgus monkey, rat, and mouse B7-H3-transfected CHO-K1 cells. DS-7300a bound to human and cynomolgus monkey 4Ig B7-H3 with similar binding affinities, but not to rat or mouse B7-H3 (Fig. 2D; Supplementary Fig. S2C; and Supplementary Table S1). DS-7300a also bound to cynomolgus monkey 2Ig B7-H3 with similar binding affinities to human 2Ig B7-H3 (Supplementary Table S1). These data suggest that the cynomolgus monkey is an appropriate species for nonclinical pharmacokinetic and toxicologic studies of DS-7300a. We confirmed the *in vitro* stability of DS-7300a in human, cynomolgus monkey, rat, and mouse plasma. The release rates of DXd from 100 µg/mL DS-7300a after a 21-day incubation ranged from 1.5% to 5.3% (Fig. 2E), indicating that DS-7300a is stable in plasma *in vitro*.

### *In vitro* cell growth inhibition by DS-7300a

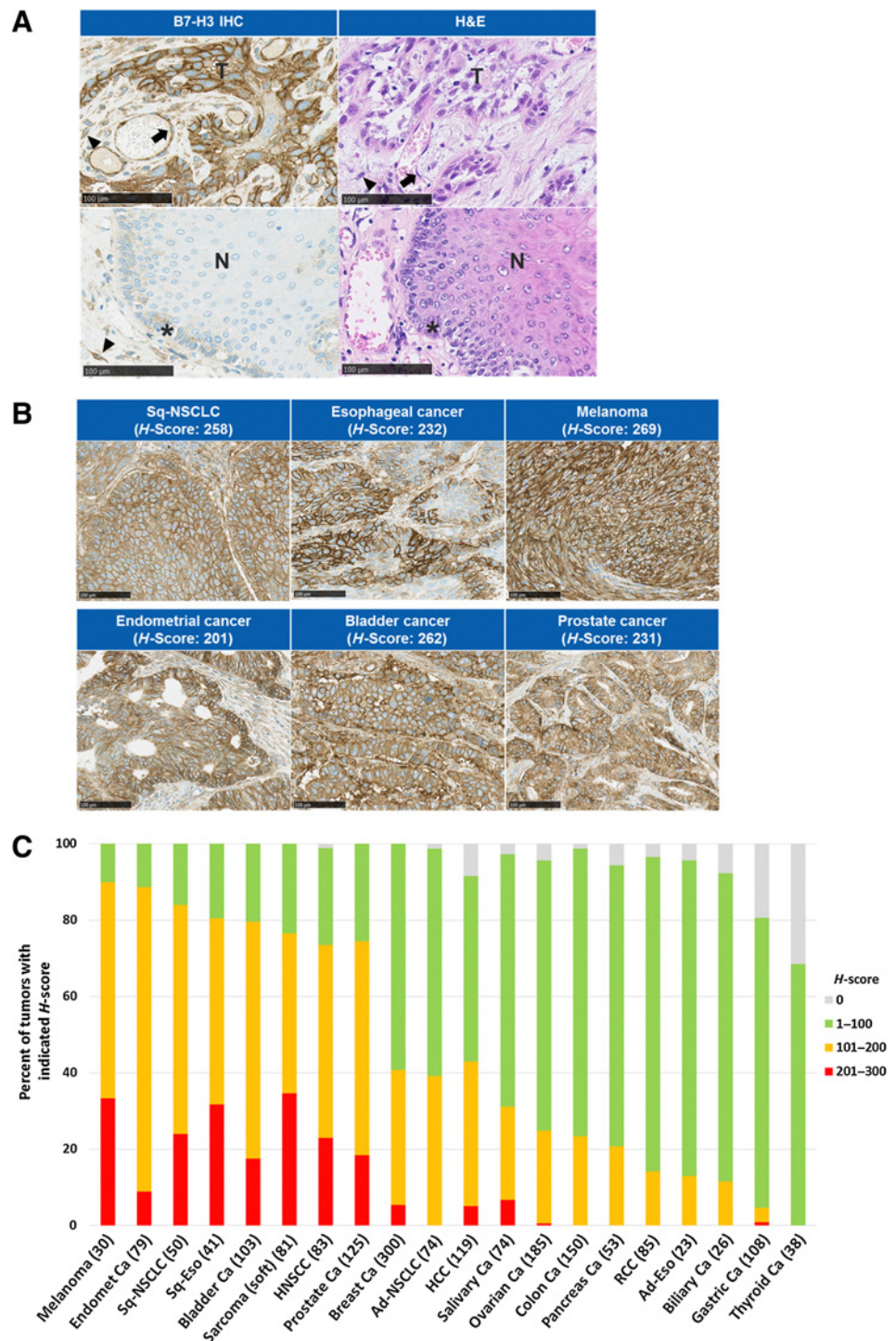
The cell growth inhibitory activity of DS-7300a was evaluated using a human rhabdomyosarcoma cell line, RH-41, a human endometrial adenocarcinoma cell line, MFE-280, and a human acute lymphocytic leukemia cell line, CCRF-CEM. Flow cytometric analysis showed that human B7-H3 was expressed on the cell surface of RH-41 and MFE-280 cells, whereas B7-H3 expression was not detected on the CCRF-CEM cells (Fig. 3A; Supplementary Table S2). DS-7300a inhibited cell growth against B7-H3-expressing RH-41 cells with an IC<sub>50</sub> value of 0.371 nmol/L (54.4 ng/mL; 95% CI, 48.1–61.6 ng/mL), and MFE-280 cells with an IC<sub>50</sub> value of 0.132 nmol/L (19.4 ng/mL; 95% CI, 17.7–21.2 ng/mL), but not against B7-H3-negative CCRF-CEM cells (Fig. 3B). Neither a parental anti-B7-H3 Ab nor isotype control ADC exhibited cell growth inhibitory activity in these cells (Fig. 3B). On the other hand, all of the cell lines tested were susceptible to DXd with IC<sub>50</sub> values of 1.00 nmol/L (95% CI, 0.915–1.09 nmol/L) for RH-41 cells, 0.357 nmol/L (95% CI, 0.311–0.409 nmol/L) for MFE-280 cells, and 0.549 nmol/L (95% CI, 0.489–0.617 nmol/L) for CCRF-CEM cells (Supplementary Fig. S3). Taken together, these results indicate that DS-7300a exhibits B7-H3-dependent cytotoxic effects *in vitro*.

### Induction of DNA damage and apoptosis in cancer cells by DS-7300a

DXd is known to induce DNA damage and lead to apoptosis in cancer cells (26, 29). To verify the contribution of DXd to the cytotoxic effect of DS-7300a, we evaluated DNA damage and apoptosis induced in RH-41 cells treated with DS-7300a, DXd, parental anti-B7-H3 Ab, and isotype control ADC. The results showed that both DS-7300a and DXd induced phosphorylation of Chk1, which is a DNA damage marker (39, 40), and cleavage of PARP, which is an apoptosis marker (41). On the other hand, parental anti-B7-H3 Ab induced neither of these (Fig. 3C). Although the isotype control ADC induced the phosphorylation of Chk1 to a lower level than that induced by DS-7300a and DXd itself, the isotype control ADC did not induce cleavage of PARP (Fig. 3C). Collectively, these results suggested that DNA damage and apoptosis in cancer cells treated with DS-7300a were caused specifically by DXd released from DS-7300a. In conclusion, the TOP1 inhibitory activity of DXd released from DS-7300a is considered to be one of the mechanisms of action for the cytotoxic effect of DS-7300a.

**Figure 1.**

IHC analysis of B7-H3 expression on human tumor tissues. **A**, Representative B7-H3 expression pattern in TMA tissue by B7-H3 IHC and image of hematoxylin and eosin (H&E) staining. Esophageal cancer (top) and normal esophagus tissue adjacent to tumor (bottom). Arrow, vasculature/endothelium; arrowhead, fibrous stromal cells; asterisk, basal cells. Scale bar, 100  $\mu$ m. **B**, Representative B7-H3 IHC images of human tumor tissues. Scale bar, 100  $\mu$ m. **C**, B7-H3 expression on various human solid tumors. B7-H3 IHC analysis was performed using TMAs. *H*-score of B7-H3 expression on tumor cells in each sample was calculated. Number in parentheses indicates the number of samples. Ad, adenocarcinoma; ca, cancer; Endomet, endometrial; Eso, esophageal cancer; HCC, hepatocellular carcinoma; HNSCC, head and neck squamous cell carcinoma; N, nontumor epithelium; RCC, renal cell carcinoma; Sq, squamous; T, tumor cells.



**In vivo antitumor activities of DS-7300a in xenograft models**

*In vivo* antitumor activities of DS-7300a were also evaluated using cell-line-derived RH-41, MEF-280, and human lung adenocarcinoma Calu-6 xenograft mouse models. As predicted from B7-H3 expression *in vitro* (Fig. 3A; Supplementary Table S2), high levels of B7-H3 expression in tumors were observed in all of the cell-line-derived xenograft models by IHC analysis. The *H*-scores of B7-H3 expression in RH-41, MFE-280, and Calu-6 tumors were 209, 151, and 180,

respectively (Fig. 4A). DS-7300a potently inhibited tumor growth even though isotype control ADC showed relatively little effect on tumor growth. DS-7300a exhibited significant antitumor activities in all of the models tested, with TGIs of 90% (3 mg/kg) and 98% (10 mg/kg) for RH-41, 67% (0.3 mg/kg), 100% (1 mg/kg), and 100% (3 mg/kg) for MFE-280, and 71% (1 mg/kg), 95% (3 mg/kg), and 99% (10 mg/kg) for Calu-6, compared with the vehicle control group at 28 days after the initial administration ( $P <$

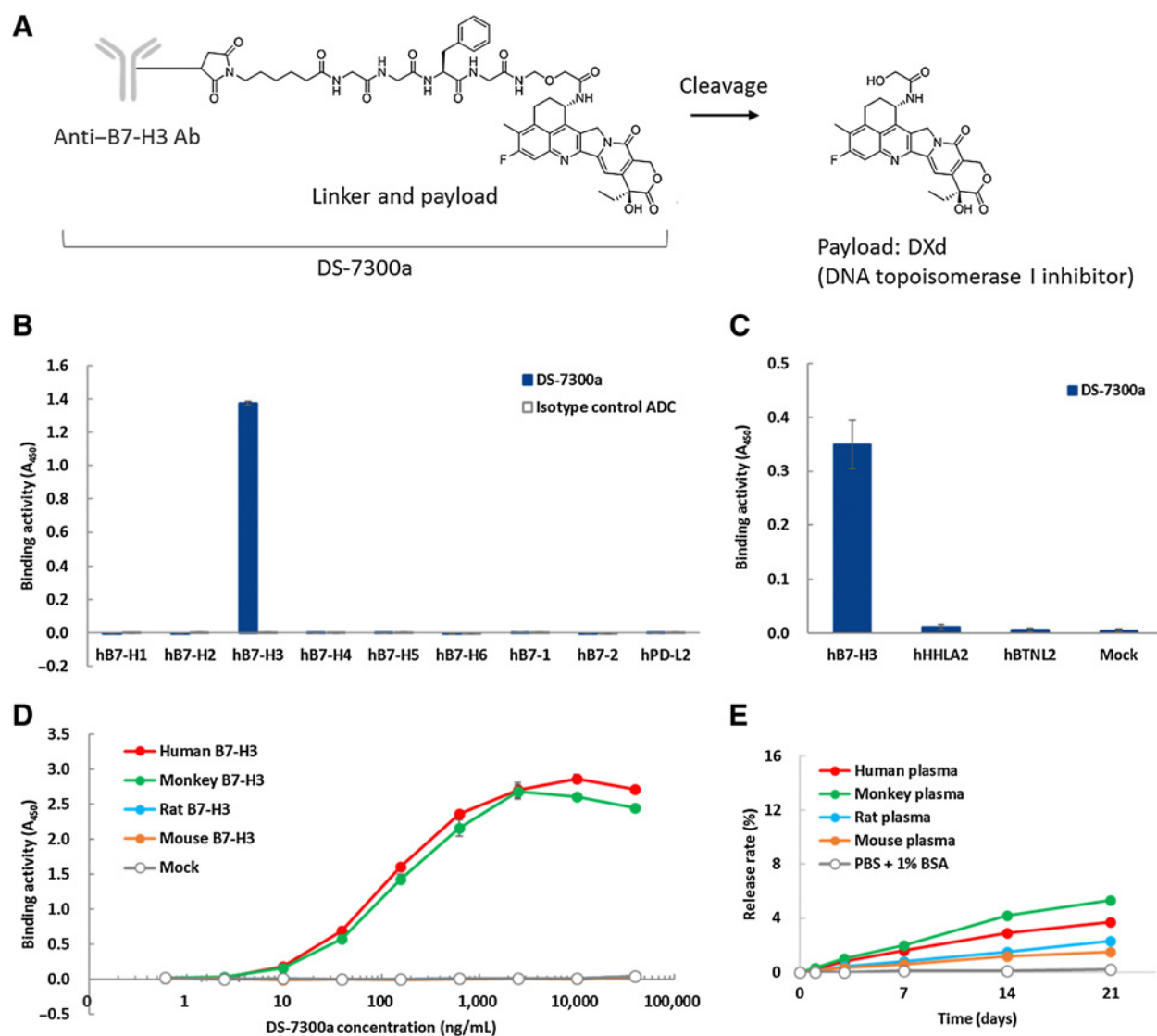


**Figure 2.**

Characteristics of DS-7300a. **A**, Schematic structure of DS-7300a. **B** and **C**, Binding activity of DS-7300a against human B7 family proteins. Recombinant proteins of human B7-H1, B7-H2, B7-H3 (4Ig), B7-H4, B7-H5, B7-H6, B7-1, B7-2, and PD-L2 were incubated with DS-7300a or isotype control ADC and binding activities were measured by ELISA. CHO-K1 cells expressing human B7-H3 (4Ig), HHLA2, and BTNL2 were incubated with DS-7300a and binding activities were measured by cell-based ELISA. Each value represents the mean and SD ( $N = 3$ ). **D**, Species cross-reactivity of DS-7300a. CHO-K1 cells expressing human (4Ig), cynomolgus monkey (4Ig), rat, and mouse B7-H3 were incubated with DS-7300a and binding activities were evaluated by cell-based ELISA. Each value represents the mean and SD ( $N = 3$ ). **E**, *In vitro* stability of DS-7300a in plasma. The release rate of DXd from 100  $\mu$ g/mL DS-7300a in human, monkey, rat, and mouse plasma was calculated using the mean concentration of the released DXd ( $N = 3$ ).

0.001; **Fig. 4A**). These results indicate that DS-7300a exhibits potent antitumor activities against B7-H3-expressing tumors through target-specific payload delivery.

To further examine the therapeutic potential of DS-7300a in more clinically relevant models, we evaluated its antitumor activities using PDX mouse models of various tumor types; human SCLC CTG-2093, human NSCLC CTG-0166, human head and neck cancer CTG-0820, and human bladder cancer CTG-1061. In all of the PDX models tested, high levels of B7-H3 expression in tumors were observed, with an *H*-score of 260 for CTG-2093, 157 for CTG-0166, 193 for CTG-0820, and 177 for CTG-1061 (**Fig. 4B**). DS-7300a showed potent and significant

antitumor activities at 10 mg/kg in all of the PDX models with TGIs of 100% for CTG-2093, 100% for CTG-0166, 97% for CTG-0820, and 88% for CTG-1061, compared with the vehicle control group at 28 days (or 22 days for CTG-1061; this shorter period was because the vehicle control group was terminated early due to the rapid growth of the tumor) after the initial administration ( $P < 0.001$  for CTG-2093 and  $P < 0.01$  for the other PDX models; **Fig. 4B**). There was no obvious body weight loss in mice treated with DS-7300a in all of the models tested in this study (Supplementary Fig. S4). These results suggest that DS-7300a has therapeutic potential against various B7-H3-expressing solid tumors.

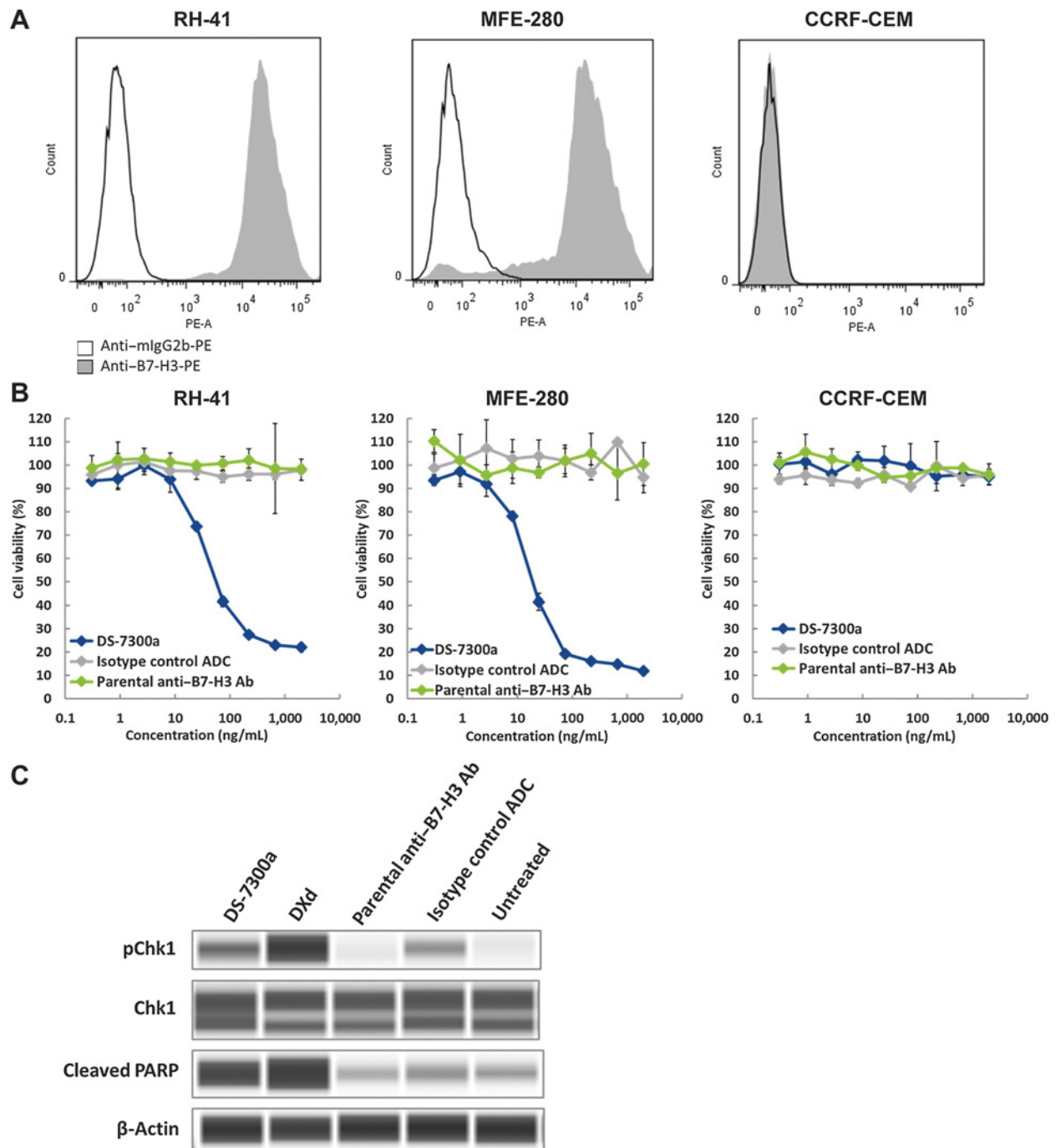


**Figure 3.** *In vitro* cytotoxic effects of DS-7300a. **A** and **B**, B7-H3 expression on human cancer cells and *in vitro* cell growth inhibition by DS-7300a. RH-41 (rhabdomyosarcoma), MFE-280 (endometrial adenocarcinoma), and CCRF-CEM (acute lymphocytic leukemia) cells were stained with PE-conjugated isotype control (mIgG2b, gray open histogram) or antihuman B7-H3 antibody (gray closed histogram) and then analyzed by flow cytometry. Cells were cultured with DS-7300a, parental anti-B7-H3 Ab, and isotype control ADC for 6 days, and then cell viability was examined. Each value represents the mean and SD ( $N = 3$ ). **C**, DNA damage and apoptosis induced by DS-7300a. RH-41 cells were treated with 10  $\mu\text{g/mL}$  DS-7300a, parental anti-B7-H3 Ab, isotype control ADC, or 10 nmol/L DXd for 72 hours. Then, the cells were harvested and analyzed by Western blotting for phosphorylated Chk1 (pChk1) as a DNA damage marker and for cleaved PARP as an apoptosis marker.

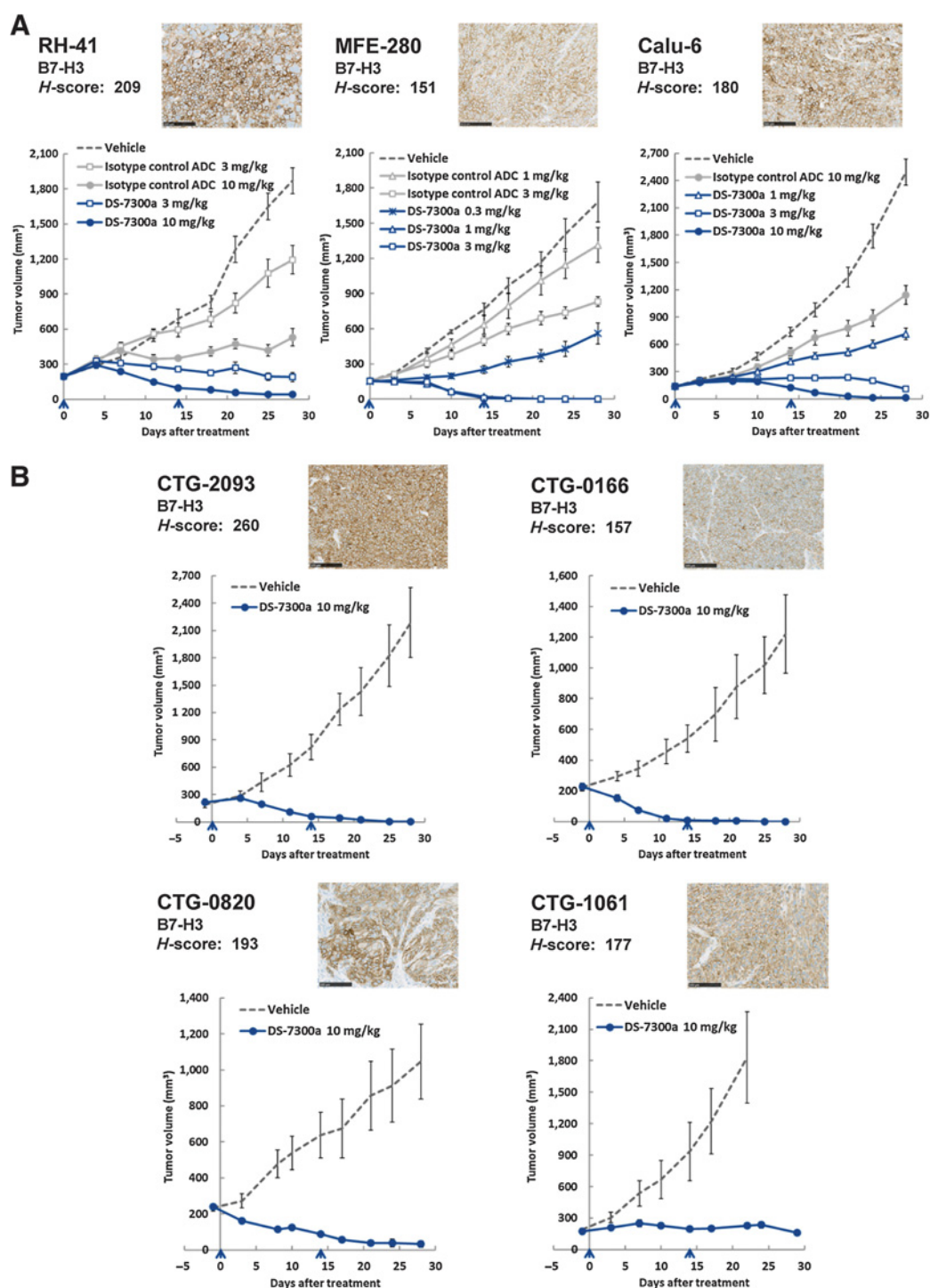


**Figure 4.**

Antitumor activities of DS-7300a in xenograft mouse models. Representative B7-H3 IHC images of tumors and *H*-scores were also shown for each model. Scale bar, 100  $\mu$ m. The indicated *H*-score represents the mean of *H*-scores in three tumor samples. The arrowhead indicates the time point of treatment. Each value represents the mean and SE of tumor volume. **A**, Antitumor activities of DS-7300a in cell line-derived xenograft models. Mice inoculated with human cancer cells, RH-41, MFE-280, or Calu-6 (NSCLC) were treated with DS-7300a, vehicle control, or isotype control ADC intravenously on days 0 and 14 ( $N = 6$  mice/group). **B**, Antitumor activities of DS-7300a in various tumor types of PDX models. PDX mice were treated with 10 mg/kg DS-7300a or vehicle control intravenously on days 0 and 14 ( $N = 5$  mice/group). CTG-2093, SCLC PDX; CTG-0166, NSCLC PDX; CTG-0820, head and neck cancer PDX; CTG-1061, bladder cancer PDX.

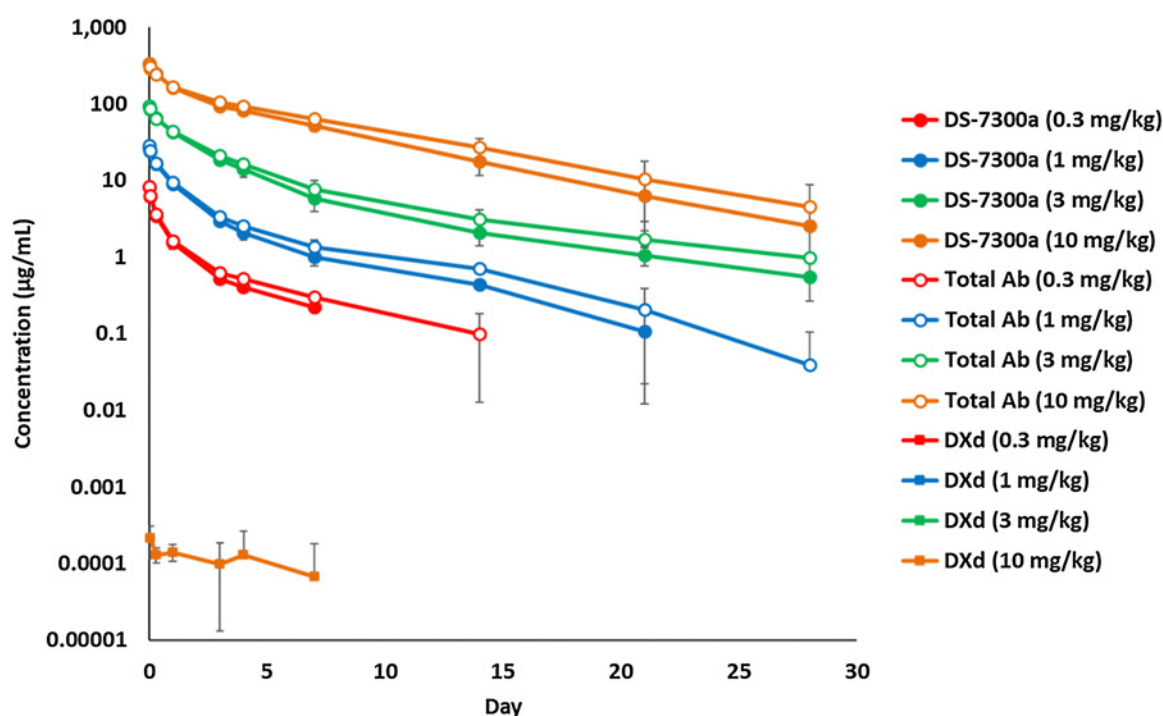


**Figure 5.**

Pharmacokinetics of DS-7300a in monkeys. DS-7300a was administered once intravenously at 0.3, 1, 3, and 10 mg/kg to cynomolgus monkeys. Plasma concentrations of DS-7300a, total Ab, and DXd were determined. Each value represents the mean and SD ( $N = 3$ ).

#### Pharmacokinetics of DS-7300a in cynomolgus monkeys

DS-7300a was administered once intravenously at 0.3, 1, 3, and 10 mg/kg to cynomolgus monkeys, and then plasma concentration of DS-7300a, total antibody, and DXd were measured up to 28 days postdose. The plasma concentration of DS-7300a increased dose-dependently. The terminal elimination half-life ( $t_{1/2}$ ) at 0.3, 1, 3, and 10 mg/kg was 3.24, 5.11, 7.89, and 4.81 days, respectively (Fig. 5; Supplementary Table S3). No clear differences in the pharmacokinetic profiles were observed between DS-7300a and the total antibody, suggesting that the linker of DS-7300a is stable in plasma *in vivo* (Fig. 5; Supplementary Table S3). Additionally, low plasma concentration of DXd was detected at the limited time points only in monkeys dosed at 10 mg/kg (Fig. 5), indicating the low systemic exposure to DXd due to the stable linker of DS-7300a and short systemic half-life of DXd.

#### Safety profiles of DS-7300a in rats and cynomolgus monkeys

To assess the general toxicity profile of DS-7300a, 1-month intermittent intravenous dose toxicity studies were conducted in cynomolgus monkeys as a cross-reactive species for DS-7300a and in rats as a non-cross-reactive species, based on the data of the species cross-reactivity of DS-7300a (Fig. 2D). A summary of repeated dose toxicity studies is shown in Table 1.

In the rat study, no animals died or showed a moribund outcome up to 200 mg/kg, the highest dose tested. In the monkey study, no death or moribund outcome was observed at any dose level throughout the study period. However, severe lung toxicity was found in one monkey at 80 mg/kg, the highest dose tested. Although the major safety concerns of TOP1 inhibitors in clinical use are gastrointestinal toxicity and bone marrow toxicity (42), no severe changes were observed in these tissues in either rats or monkeys, with the very slight histopath-

ologic findings of single cell necrosis in the crypt epithelium in the small and/or large intestines, and no abnormal changes in the bone marrow in monkeys. Taking the findings together, the severely toxic dose in 10% of the animals ( $STD_{10}$ ) was determined to be greater than 200 mg/kg for rats, and the highest nonseverely toxic dose (HNSTD) in cynomolgus monkeys was considered to be 30 mg/kg. DS-7300a was well tolerated in rats and monkeys in the 1-month intermittent dose toxicity study.

## Discussion

Here, we report the development of DS-7300a, a potent TOP1 inhibitor, DXd-based ADC targeting B7-H3. DS-7300a exhibited DXd-derived antitumor activities against B7-H3-expressing tumors in preclinical models and acceptable safety profiles in monkeys.

DS-7300a utilizes the same linker-payload technology as trastuzumab deruxtecan, the HER2-targeting ADC which is recently approved for treating adult patients with HER2-positive breast and gastric cancers. DS-7300a was designed to have a DAR of 4 on average to maintain a better safety margin with reference to the knowledge of datopotamab deruxtecan, a TROP2-targeting ADC (30). As expected, DS-7300a strongly inhibited tumor growth *in vivo*, was stable in monkey plasma *in vitro* and *in vivo*, and was well tolerated in monkeys.

DS-7300a inhibited the growth of B7-H3-expressing cancer cells but not that of B7-H3-negative cancer cells *in vitro*, although all of the cells tested were sensitive to the free payload DXd itself. In addition, the changes in DNA damage and apoptosis markers resulted by DS-7300a or relevant controls in B7-H3-expressing RH-41 cells suggest that DS-7300a exerts cytotoxic effects through the TOP1 inhibitory activity of DXd released from DS-7300a. In the evaluation of the antitumor activities of DS-7300a in cell-line-derived xenograft models, DS-7300a

**Table 1.** Summary of repeated dose toxicity studies in rats and monkeys.

Species	CrI:CD(SD) rats	Cynomolgus monkeys
Regimens	0, 20, 60, and 200 mg/kg Intravenous, every 2 weeks for 4 weeks (3 times in total)	0, 10, 30, and 80 mg/kg Intravenous, every 2 weeks for 4 weeks (3 times in total)
Animals (N)	10/sex/group (main): all dose groups 5/sex/group (recovery): 0 and 200 mg/kg	3/sex/group (main): all dose groups 2/sex/group (recovery): all dose groups
Lethal dose	>200 mg/kg	>80 mg/kg
Body weight	≤60 mg/kg: normal 200 mg/kg: decreased	≥10 mg/kg: decreased (slight and transient)
Urinalysis	≤60 mg/kg: normal 200 mg/kg: increased protein	≤80 mg/kg: normal
Hematology	≤60 mg/kg: normal 200 mg/kg: decreased WBC, LYM, and NEU, increased monocytes	≥10 mg/kg: decreased RBC, Hb, Ht 80 mg/kg: increased PLT and fibrinogen
Blood chemistry	≤60 mg/kg: normal 200 mg/kg: increased UN	≤30 mg/kg: normal 80 mg/kg: decreased albumin
Target organs and tissues	≥20 mg/kg: intestine ≥60 mg/kg: bone marrow 200 mg/kg: kidney, skin, testis, thymus, tooth (incisor) No severe change. All changes reversible except in the testis.	≥10 mg/kg: intestine, skin (injection site) ≥30 mg/kg: skin 80 mg/kg: kidney, lung, thymus No severe change except in the lungs. All changes slight and reversible except in the lungs.
STD <sub>10</sub> /HNSTD	STD <sub>10</sub> : >200 mg/kg	HNSTD: 30 mg/kg

Abbreviations: Hb, hemoglobin; Ht, hematocrit; LYM, lymphocyte; NEU, neutrophil; PLT, platelet; RBC, red blood cell; UN, urea nitrogen; WBC, white blood cell.

exhibited potent antitumor activities of tumor regression against the high-B7-H3 models tested in this study. In these models, isotype control ADC also showed nonspecific antitumor activities, but they were much lower than those by DS-7300a at the same dose levels, suggesting that DS-7300a demonstrated B7-H3-dependent antitumor activities *in vivo*. In the MFE-280 xenograft model, DS-7300a exhibited potent antitumor activities with TGI of 100% at 1 and 3 mg/kg, low doses compared with those in the other high-B7-H3 models. In addition, MFE-280 cells were highly susceptible to DXd *in vitro*, suggesting that the variation of DXd sensitivity among the cell lines may affect the antitumor activities of DS-7300a. Further investigation including less sensitive cell lines to DXd will help us to understand the importance of payload sensitivity in antitumor activity of DS-7300a.

We confirmed the high level of B7-H3 expression in various types of solid tumors in the TMAs. Therefore, the PDX mouse model studies in NSCLC, SCLC, head and neck cancer, and bladder cancer were performed to examine the therapeutic potential of DS-7300a in more clinically relevant tumor models. DS-7300a exerted potent antitumor activities in these high-B7-H3-expressing PDX models. To understand a correlation between the efficacy of DS-7300a and B7-H3 expression, further comprehensive analysis using PDX models with various B7-H3 expression levels will be required. In addition to B7-H3 expression on tumor cells, other factors may also contribute to the sensitivity of DS-7300a. For instance, overexpression of drug efflux transporters, lack of expression of a restriction factor for replicative stress, Schlafen 11 (SLFN 11), and low expression or inactivation of lysosomal enzymes might also affect susceptibility to DS-7300a (24, 42, 43). Further mechanistic analysis will help us to better understand the factors conferring sensitivity to DS-7300a. B7-H3 is expressed not only in tumor cells but also in stromal cells such as tumor endothelial cells and fibroblasts in tumor tissues. Thus, DS-7300a may exert more potent antitumor activities in humans by targeting not only B7-H3-expressing tumor cells but also B7-H3-expressing stromal cells in tumor tissues (14). Since DS-7300a does not bind to mouse B7-H3, the effect of DS-7300a on the mouse-derived stromal cells in xenograft tumors could not be evaluated in the xenograft studies. Moreover, the released DXd shows bystander antitumor activity on

neighboring cells in tumor tissues due to its high membrane permeability (31) which may be expected to extend antitumor activity of DS-7300a even in heterogeneous tumor tissues. Further comprehensive analysis using patient tissue samples obtained from the ongoing clinical study of DS-7300a will be required to understand the DS-7300a antitumor activity in humans. In this study, we did not examine the contribution of DS-7300a to antitumor immunity, although B7-H3 has been reported to be an immune checkpoint molecule (2, 6). Further investigation may be warranted to elucidate the potential immune effect of DS-7300a for cancer immunotherapy.

DS-7300a showed acceptable pharmacokinetic profiles in monkeys, the cross-reactive species. Although the total body clearance (CL) of DS-7300a might be affected by target mediated drug disposition (TMDD) due to the distribution of DS-7300a to B7-H3-expressing nontumor cells such as stromal cells, the CL values were decreased in dose-dependent manner, and TMDD seemed to be almost saturated at the higher doses, which are supposed to be the clinically relevant doses. Further analysis will be required to compare pharmacokinetics between humans and monkeys.

In the toxicity study, DS-7300a showed an acceptable safety profile in monkeys. The HNSTD in monkeys was considered to be 30 mg/kg since severe lung toxicity was observed in one monkey at 80 mg/kg, the highest dose tested. It has been reported that B7-H3 expression is almost undetectable in normal human lungs (14, 17); however, B7-H3 expression in the monkey lungs is still unclear. Further evaluation is necessary to elucidate the mode of mechanisms of the lung toxicity related to DS-7300a in monkeys. In the studies of trastuzumab deruxtecan, lung toxicity in monkeys (26, 27, 44) and interstitial lung diseases (ILD)/pneumonitis related to trastuzumab deruxtecan in humans (33–38) were observed. Therefore, careful safety monitoring in humans is required in clinical study of DS-7300a.

In summary, we generated a novel B7-H3-targeting ADC conjugated with the potent TOP1 inhibitor DXd, DS-7300a. DS-7300a exerted potent antitumor activities in high-B7-H3-expressing tumors in preclinical models including PDX mouse models through B7-H3-specific payload delivery. Furthermore, DS-7300a

showed acceptable pharmacokinetic and safety profiles in monkeys. Accordingly, DS-7300a may be effective in treating patients with B7-H3-expressing solid tumors. A first-in-human phase I/II study of DS-7300a in patients with advanced solid tumors is currently in progress (NCT04145622).

### Authors' Disclosures

Dr. Y. Abe reports a patent for ANTIBODY-DRUG CONJUGATE issued to Daiichi Sankyo., Ltd. T. Nakada reports a patent for ANTIBODY-DRUG CONJUGATE issued to Daiichi Sankyo Co., Ltd. No disclosures were reported by the other authors.

### Authors' Contributions

**M. Yamato:** Conceptualization, resources, data curation, formal analysis, validation, investigation, visualization, methodology, writing—original draft, project administration, writing—review and editing. **J. Hasegawa:** Resources, formal analysis, validation, investigation, visualization, methodology, writing—original draft, writing—review and editing. **T. Maejima:** Resources, data curation, formal analysis, validation, investigation, visualization, methodology, writing—original draft, writing—review and editing. **C. Hattori:** Resources, data curation, formal analysis, validation, investigation, visualization, writing—review and editing. **K. Kumagai:** Resources, data curation, formal analysis, validation, investigation, visualization, methodology, writing—original draft, writing—review and editing. **A. Watanabe:** Resources, data curation,

formal analysis, validation, investigation, visualization, methodology, writing—original draft, writing—review and editing. **Y. Nishiyama:** Formal analysis, visualization, writing—review and editing. **T. Shibutani:** Resources, formal analysis, validation, investigation, visualization, methodology, writing—review and editing. **T. Aida:** Resources, formal analysis, validation, investigation, visualization, methodology, writing—review and editing. **I. Hayakawa:** Resources, validation, investigation, visualization, methodology, writing—review and editing. **T. Nakada:** Resources, validation, investigation, visualization, methodology, writing—review and editing. **Y. Abe:** Conceptualization, supervision, methodology, project administration. **T. Agatsuma:** Conceptualization, supervision, methodology, project administration.

### Acknowledgments

Human TMAs were provided from University Hospital Basel, Switzerland. The authors thank Hironobu Komori and Yasuko Otsuka for their contributions to the data generation. They also thank Nanae Izumi, Tsuneo Deguchi, Max Qian, and all of the team members for providing their expertise and assistance in the preclinical studies.

The costs of publication of this article were defrayed in part by the payment of page charges. This article must therefore be hereby marked *advertisement* in accordance with 18 U.S.C. Section 1734 solely to indicate this fact.

Received June 23, 2021; revised November 12, 2021; accepted February 7, 2022; published first February 11, 2022.

### References

- Chapoval AI, Ni J, Lau JS, Wilcox RA, Flies DB, Liu D, et al. B7-H3: a costimulatory molecule for T cell activation and IFN- $\gamma$  production. *Nat Immunol* 2001;2:269–74.
- Schildberg FA, Klein SR, Freeman GJ, Sharpe AH. Coinhibitory pathways in the B7-CD28 ligand-receptor family. *Immunity* 2016;44:955–72.
- Sun M, Richards S, Prasad DVR, Mai XM, Rudensky A, Dong C. Characterization of mouse and human B7-H3 genes. *J Immunol* 2002; 168:6294–7.
- Ling V, Wu PW, Spaulding V, Kieleczawa J, Luxenberg D, Carreno BM, et al. Duplication of primate and rodent B7-H3 immunoglobulin V- and C-like domains: divergent history of functional redundancy and exon loss. *Genomics* 2003;82:365–77.
- Steinberger P, Majdic O, Derdak SV, Pfistershammer K, Kirchberger S, Klauser C, et al. Molecular characterization of human 4Ig-B7-H3, a member of the B7 family with four Ig-like domains. *J Immunol* 2004;172:2352–9.
- Kontos F, Michelakos T, Kurokawa T, Sadagopan A, Schwab JH, Ferrone CR, et al. B7-H3: an attractive target for antibody-based immunotherapy. *Clin Cancer Res* 2021;27:1227–35.
- Inamura K, Yokouchi Y, Kobayashi M, Sakakibara R, Ninomiya H, Subat S, et al. Tumor B7-H3 (CD276) expression and smoking history in relation to lung adenocarcinoma prognosis. *Lung Cancer* 2017;103:44–51.
- Yonesaka K, Haratani K, Takamura S, Sakai H, Kato R, Takegawa N, et al. B7-H3 negatively modulates CTL-mediated cancer immunity. *Clin Cancer Res* 2018;24: 2653–64.
- Song J, Shi W, Zhang Y, Sun M, Liang X, Zheng S. Epidermal growth factor receptor and B7-H3 expression in esophageal squamous tissues correlate to patient prognosis. *Oncol Targets Ther* 2016;9:6257–63.
- Brunner A, Hinterholzer S, Riss P, Heinze G, Brustmann H. Immunoreexpression of B7-H3 in endometrial cancer: relation to tumor T-cell infiltration and prognosis. *Gynecol Oncol* 2012;124:105–11.
- Zang X, Thompson RH, Al-Ahmadie HA, Serio AM, Reuter VE, Eastham JA, et al. B7-H3 and B7x are highly expressed in human prostate cancer and associated with disease spread and poor outcome. *Proc Natl Acad Sci U S A* 2007;104:19458–63.
- Maeda N, Yoshimura K, Yamamoto S, Kuramasu A, Inoue M, Suzuki N, et al. Expression of B7-H3, a potential factor of tumor immune evasion in combination with the number of regulatory T cells, affects against recurrence-free survival in breast cancer patients. *Ann Surg Oncol* 2014; 21:546–54.
- Zhang X, Fang C, Zhang G, Jiang F, Wang L, Hou J. Prognostic value of B7-H3 expression in patients with solid tumors: a meta-analysis. *Oncotarget* 2017;8: 93156–67.
- Seaman S, Zhu Z, Saha S, Zhang XM, Yang MY, Hilton MB, et al. Eradication of tumors through simultaneous ablation of CD276/B7-H3-positive tumor cells and tumor vasculature. *Cancer Cell* 2017;31:501–15.
- Seaman S, Stevens J, Yang MY, Logsdon D, Graff-Cherry C, St. Croix B. Genes that distinguish physiological and pathological angiogenesis. *Cancer Cell* 2007; 11:539–54.
- Xu H, Cheung IY, Guo HF, Cheung NKV. MicroRNA miR-29 modulates expression of immunoinhibitory molecule B7-H3: potential implications for immune based therapy of human solid tumors. *Cancer Res* 2009;69: 6275–81.
- Du H, Hirabayashi K, Ahn S, Kren NP, Montgomery SA, Wang X, et al. Antitumor responses in the absence of toxicity in solid tumors by targeting B7-H3 via chimeric antigen receptor T cells. *Cancer Cell* 2019; 35:221–37.
- Zhou X, Ouyang S, Li J, Huang X, Ai X, Zeng Y, et al. The novel non-immunological role and underlying mechanisms of B7-H3 in tumorigenesis. *J Cell Physiol* 2019;234:21785–95.
- Husain B, Ramani SR, Chiang E, Lehoux I, Paduchuri S, Arena TA, et al. A platform for extracellular interactome discovery identifies novel functional binding partners for the immune receptors B7-H3/CD276 and PVR/CD155. *Mol Cell Proteomics* 2019;18:2310–23.
- Nagase-Zembutsu A, Hirotsu K, Yamato M, Yamaguchi J, Takata T, Yoshida M, et al. Development of DS-5573a: a novel afucosylated mAb directed at B7-H3 with potent antitumor activity. *Cancer Sci* 2016;107: 674–81.
- Loo D, Alderson RF, Chen FZ, Huang L, Zhang W, Gorlatov S, et al. Development of an Fc-enhanced anti-B7-H3 monoclonal antibody with potent antitumor activity. *Clin Cancer Res* 2012;18:3834–45.
- Majzner RG, Theruvath JL, Nellan A, Heitzeneder S, Cui Y, Mount CW, et al. CAR T cells targeting B7-H3, a pan-cancer antigen, demonstrate potent preclinical activity against pediatric solid tumors and brain tumors. *Clin Cancer Res* 2019;25:2560–74.
- Scribner JA, Brown JG, Son T, Chiechi M, Li P, Sharma S, et al. Preclinical development of MGC018, a duocarmycin-based antibody-drug conjugate targeting B7-H3 for solid cancer. *Mol Cancer Ther* 2020;19:2235–44.

24. Hafeez U, Parakh S, Gan HK, Scott AM. Antibody-drug conjugates for cancer therapy. *Molecules* 2020;25:4764.
25. Nakada T, Masuda T, Naito H, Yoshida M, Ashida S, Morita K, et al. Novel antibody drug conjugates containing exatecan derivative-based cytotoxic payloads. *Bioorganic Med Chem Lett* 2016;26:1542–5.
26. Ogitan Y, Aida T, Hagihara K, Yamaguchi J, Ishii C, Harada N, et al. DS-8201a, a novel HER2-targeting ADC with a Novel DNA topoisomerase I inhibitor, demonstrates a promising antitumor efficacy with differentiation from T-DM1. *Clin Cancer Res* 2016;22:5097–108.
27. Nakada T, Sugihara K, Jikoh T, Abe Y, Agatsuma T. The latest research and development into the antibody–drug conjugate, [fam-] trastuzumab deruxtecan (DS-8201a), for HER2 cancer therapy. *Chem Pharm Bull* 2019;67:173–85.
28. Hashimoto Y, Koyama K, Kamai Y, Hirotsu K, Ogitan Y, Zembutsu A, et al. A novel HER3-targeting antibody–drug conjugate, U3–1402, exhibits potent therapeutic efficacy through the delivery of cytotoxic payload by efficient internalization. *Clin Cancer Res* 2019;25:7151–61.
29. Iida K, Abdelhamid Ahmed AH, Nagatsuma AK, Shibutani T, Yasuda S, Kitamura M, et al. Identification and therapeutic targeting of GPR20, selectively expressed in gastrointestinal stromal tumors, with DS-6157a, a first-in-class antibody–drug conjugate. *Cancer Discov* 2021;11:1508–23.
30. Okajima D, Yasuda S, Maejima T, Karibe T, Sakurai K, Aida T, et al. Datopitamab deruxtecan, a novel TROP2-directed antibody–drug conjugate, demonstrates potent antitumor activity by efficient drug delivery to tumor cells. *Mol Cancer Ther* 2021;20:2329–40.
31. Ogitan Y, Hagihara K, Oitate M, Naito H, Agatsuma T. Bystander killing effect of DS-8201a, a novel anti-human epidermal growth factor receptor 2 antibody–drug conjugate, in tumors with human epidermal growth factor receptor 2 heterogeneity. *Cancer Sci* 2016;107:1039–46.
32. Doi T, Shitara K, Naito Y, Shimomura A, Fujiwara Y, Yonemori K, et al. Safety, pharmacokinetics, and antitumor activity of trastuzumab deruxtecan (DS-8201), a HER2-targeting antibody–drug conjugate, in patients with advanced breast and gastric or gastro-oesophageal tumours: a phase 1 dose-escalation study. *Lancet Oncol* 2017;18:1512–22.
33. Tamura K, Tsurutani J, Takahashi S, Iwata H, Krop IE, Redfern C, et al. Trastuzumab deruxtecan (DS-8201a) in patients with advanced HER2-positive breast cancer previously treated with trastuzumab emtansine: a dose-expansion, phase 1 study. *Lancet Oncol* 2019;20:816–26.
34. Shitara K, Iwata H, Takahashi S, Tamura K, Park H, Modi S, et al. Trastuzumab deruxtecan (DS-8201a) in patients with advanced HER2-positive gastric cancer: a dose-expansion, phase 1 study. *Lancet Oncol* 2019;20:827–36.
35. Modi S, Saura C, Yamashita T, Park YH, Kim S-B, Tamura K, et al. Trastuzumab deruxtecan in previously treated HER2-positive breast cancer. *N Engl J Med* 2020;382:610–21.
36. Tsurutani J, Iwata H, Krop IE, Jänne PA, Doi T, Takahashi S, et al. Targeting HER2 with trastuzumab deruxtecan: a dose-expansion, phase I study in multiple advanced solid tumors. *Cancer Discov* 2020;10:688–701.
37. Shitara K, Bang Y-J, Iwasa S, Sugimoto N, Ryu M-H, Sakai D, et al. Trastuzumab deruxtecan in previously treated HER2-positive gastric cancer. *N Engl J Med* 2020;382:2419–30.
38. Siena S, Di Bartolomeo M, Raghav K, Masuishi T, Loupakis F, Kawakami H, et al. Trastuzumab deruxtecan (DS-8201) in patients with HER2-expressing metastatic colorectal cancer (DESTINY-CRC01): a multicentre, open-label, phase 2 trial. *Lancet Oncol* 2021;22:779–89.
39. Zhao H, Piwnicka-Worms H. ATR-mediated checkpoint pathways regulate phosphorylation and activation of human Chk1. *Mol Cell Biol* 2001;21:4129–39.
40. Xiao Z, Chen Z, Gunasekera AH, Sowin TJ, Rosenberg SH, Fesik S, et al. Chk1 mediates S and G2 arrests through Cdc25A degradation in response to DNA-damaging agents. *J Biol Chem* 2003;278:21767–73.
41. Kaufmann SH, Desnoyers S, Ottaviano Y, Davidson NE, Poirier GG. Specific proteolytic cleavage of Poly(ADP-ribose) polymerase: an early marker of chemotherapy-induced apoptosis. *Cancer Res* 1993;53:3976–85.
42. Thomas A, Pommier Y. Targeting topoisomerase I in the era of precision medicine. *Clin Cancer Res* 2019;25:6581–9.
43. Zoppoli G, Regairaz M, Leo E, Reinhold WC, Varma S, Ballestrero A, et al. Putative DNA/RNA helicase Schlafen-11 (SLFN11) sensitizes cancer cells to DNA-damaging agents. *Proc Natl Acad Sci U S A* 2012;109:15030–5.
44. Kumagai K, Aida T, Tsuchiya Y, Kishino Y, Kai K, Mori K. Interstitial pneumonitis related to trastuzumab deruxtecan, a human epidermal growth factor receptor 2-targeting Ab–drug conjugate, in monkeys. *Cancer Sci* 2020;111:4636–45.